

Laser - BNSiO₂ Ceramics Interaction: simulation of the energy deposition on dielectric wall surfaces in Hall thrusters

C. FOCSA^{a*}, M. ZISKIND^a, C. URSU^{a,b}, S. GURLUI^b, D. PAGNON^c, S. PELLERIN^d, N. PELLERIN^e, M. DUDECK^f

^a*Laboratoire de Physique des Lasers, Atomes et Molécules (UMR CNRS 8523), Centre d'Etudes et de Recherches Lasers et Applications (FR CNRS 2416), Université de Lille 1, 59655 Villeneuve d'Ascq, France*

^b*Universitatea "Al. I. Cuza", Iasi-700506, Romania*

^c*Laboratoire de Physique des Gaz et des Plasmas, Université de Paris XI, 91405 Orsay, France*

^d*Laboratoire d'Analyse Spectroscopique et d'Energétique des Plasmas, 18028 Bourges, Université d'Orléans, France*

^e*Centre de Recherche sur les Matériaux à Hautes Température, 45071 Orléans, France*

^f*Laboratoire ICARE, CNRS Orléans, 45071 Orléans, France*

The dielectric wall surfaces of the annular chamber which are used in Hall Effect Thrusters (HET) to limit the plasma discharge play an important role but yet completely not understood and controlled. In order to investigate the effect of an energy flux on the wall we performed tests with a nanosecond pulsed laser to simulate the energy deposition on BNSiO₂ (usual dielectric material for HETs). The tests have been carried out with the second harmonic (532 nm) of a Q-switched (10 ns) Nd:YAG laser focused on the samples placed in a vacuum chamber (10⁻⁶ Torr). The energy/pulse range explored has been 5 – 320 mJ, leading to fluences of 1 – 1000 J/cm². The modifications induced by laser irradiation on the BNSiO₂ targets have been analysed by profilometry and scanning electron microscopy. The plasma created by laser ablation has also been characterized by optical and spectral methods. The present paper presents preliminary results of these combined investigations.

(Received February 16, 2008; accepted August 14, 2008)

Keywords: BNSiO₂, Ceramics, Laser interaction, Hall thrusters, Simulation

1. Introduction

Last decades have seen the appearance of new techniques based on the laser–solid matter interaction, like matrix-assisted laser desorption and ionization [1,2] (MALDI), pulsed laser deposition, [3] or dry laser cleaning [4] (DLC). There is therefore a high current interest in a better understanding of the fundamentals of the photo-excited processes on multi-component samples, in order to fully exploit (and possibly extend) their technological and analytical capabilities. A thorough investigation of the complex laser–sample interaction seems necessary, in terms of ejected products, nature of the desorption process itself, and/or the specific response to different parameters involved, like pulse energy or wavelength of the exciting laser beam. In this frame, a combined analysis of the modifications induced on the solid sample by laser irradiation and of the properties and dynamics of the ejected gas phase can offer valuable insights for a more complete view of the desorption/ablation phenomena and for the behavior of specific materials under high fluence photon excitation.

The BNSiO₂ ceramics used in this study represents the typical material employed in the manufacturing of the dielectric walls of the Hall Effect Thrusters (HET) annular chamber. [5,6] The presence of numerous complex processes like electron secondary emission, sputtering,

normal or ab-normal erosion, [7-9] sheath potential modifications or solid particle emission turns the efforts to completely control and parameterize the dielectric wall behaviour into a difficult task. Moreover, the deposition of energy by the plasma discharge modifies the surface temperature and consequently affects the evolution of the different wall processes.

In order to better understand the effects of an energy flux on the wall, we try to simulate the energy deposition by irradiating the BNSiO₂ surface with a nanosecond pulsed laser. A collaborative network has been established between several laboratories in order to achieve a characterization as complete as possible of the effects of photon energy deposition on the solid ceramics samples. This has been done by a variety of techniques, addressing the solid phase (profilometry at LPGP in Orsay, or scanning electron microscopy at CRMHT in Orléans), but also the ejected gas phase, by optical and spectral investigations of the plasma plume in PhLAM laboratory (Villeneuve d'Ascq). The present paper aims to describe the capabilities of these various analytical techniques by presenting a panel of representative preliminary results rather than giving definitive statements on the interpretation of the multifaceted and intricate processes involved.

2. Experimental set-up

The experimental technique is based on a set-up (see Fig. 1 for a schematic view) developed mainly for analytical purposes and described in detail elsewhere [10-12]. The experiments have been performed in a 10 l stainless steel vacuum chamber evacuated by means of a 450 l/s turbomolecular pump (Varian) to a base pressure $< 10^{-6}$ Torr. The second harmonic ($\lambda = 532$ nm) of a Q-switched 10 ns Nd:YAG laser (Quantel) has been focused at normal incidence by a $f = 25$ cm lens on the BNSiO₂ target placed in the vacuum chamber. The samples (20 mm diameter, 2 mm thick flat disks) have been placed on a micrometric XYZ positioning system, allowing the exposure of different spots on the same sample surface. The laser beam energy (5-320 mJ/pulse) has been continuously monitored by an OPHIR joulemeter.

Two main groups of experiments have been performed: the first one dealt with irradiation of BNSiO₂ samples for further ex-situ measurements (profilometry, scanning electron microscopy) of the affected solid phase, while the second one was dedicated to the in-situ study of the plasma plume created by laser ablation. For the first set of experiments, the protocol we adopted was to irradiate each sample spot with 100 laser pulses (10 s at 10 Hz). For the second set, different irradiation times have been used, from shot-to-shot to several thousands shots applied to the same spot.

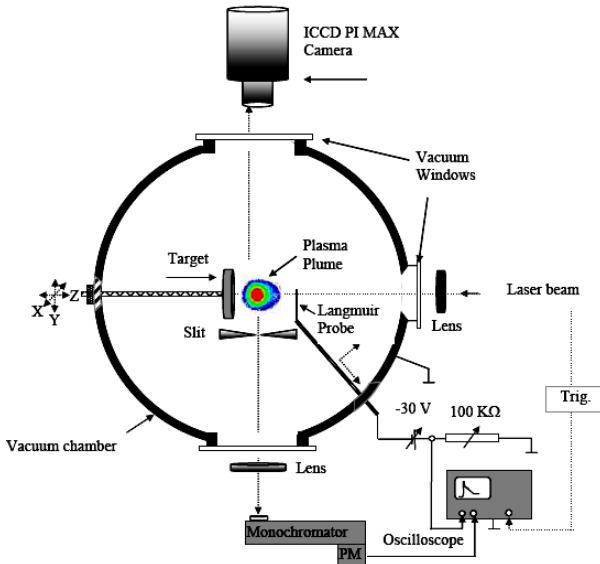


Fig. 1. Schematic view of the laser ablation experimental set-up.

The formation and dynamics of the plasma plume have been studied by means of an intensified CCD camera (Princeton Instruments, 576X384 pixels, gating time 20 ns) placed orthogonally to the plasma expansion direction. A Nikon lens has been used to image the plume onto the camera. A 25 cm Jobin-Yvon monochromator and a fast response photomultiplier (Hamamatsu) have been used to spectrally resolve the UV-visible emission of the plume. Different slices of the plasma (along the Z axis) have been selected by a slit (1 mm width) placed in the vacuum

chamber (see Fig. 1). A cylindrical Langmuir probe (stainless steel 0.8 mm diameter, 5 mm length), biased at -30 V (stabilized dc power source) and placed at 18.5 mm from the target can be used to record the total ionic current generated by the plasma expansion. The transitory signals have been recorded by a 2 GHz digital oscilloscope (LeCroy WaveRunner 6200A) and transferred to a PC for further analysis (LabView environment).

3. Results and discussion

3.1 Sample modifications induced by laser irradiation

Fig. 2 presents a series of spots irradiated at various laser fluences and exposure times, when translating the sample at different positions in the XY plane. A quick visual inspection allows one to conclude on the important modifications induced on the sample by the laser beam. The next step has been to perform a systematic study of these modifications as a function of the laser parameters. Profilometric measurements have been done in the LPGP laboratory (Orsay) in order to estimate the depth ablated per laser shot for further comparison with the conditions observed on working cycles of HETs.

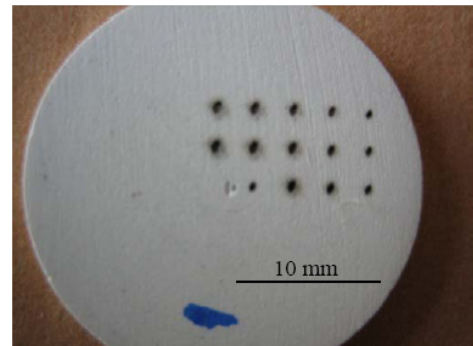
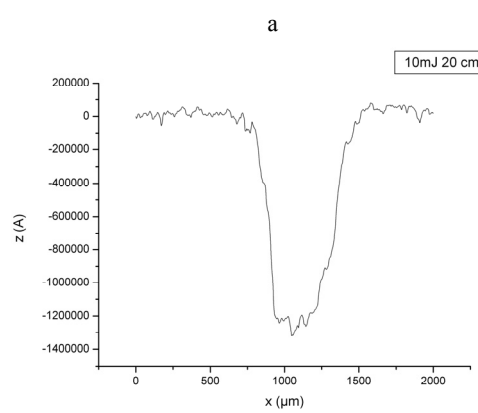
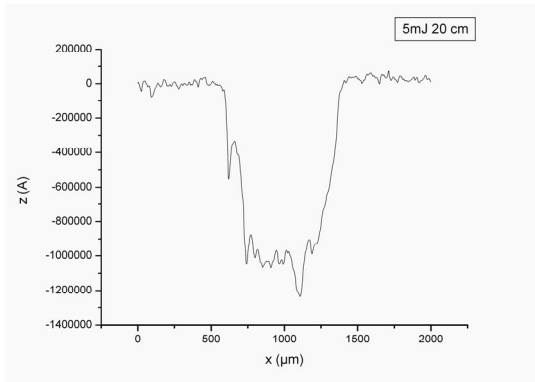


Fig. 2. Impact spots on the BNSiO₂ sample surface for various laser fluences and exposure times.

The results presented in Fig. 3 (a-c) show a rather slow increase of the ablated depth with the pulse energy. A preliminary fit using laser fluences in the range 0 – 30 J/cm² (this spans the energy range from 5 to 240 mJ/pulse, with typical values of the crater diameter of 0.6 – 1 mm, and ablation rates of 1 to 2 $\mu\text{m/laser pulse}$) gives a “classical” logarithmic dependence of the ablated depth with the fluence [13]:

$$z = z_0 \ln(F/F_{\text{th}}) \quad (1)$$

where F_{th} stands for the threshold fluence, and z_0 is a characteristic ablation rate, usually related to the optical absorption coefficient of the sample. With the data in Fig. 4, we found a threshold fluence of ~ 50 mJ/cm² (this turns into a threshold energy of 0.2 mJ/pulse for a typical 0.7 mm diameter crater) and a characteristic ablation rate of 0.32 $\mu\text{m/laser shot}$.



b

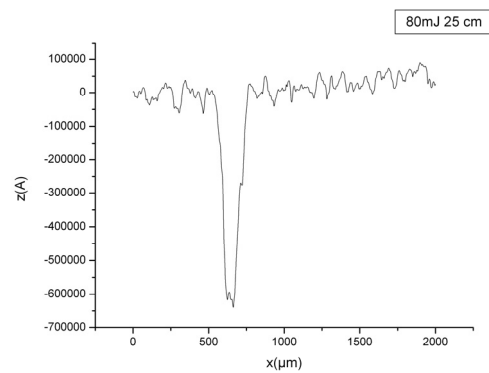
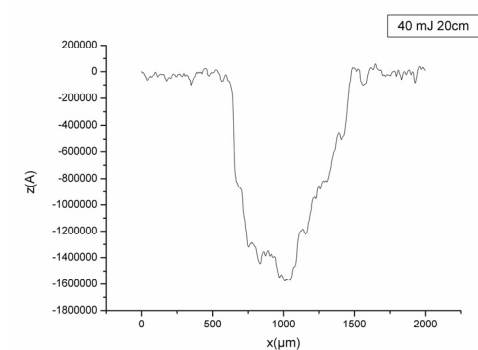


Fig. 3. Profilometric measurements of the craters created by laser ablation on a BNSiO_2 sample. 100 laser pulses have been used for each experiment. The laser pulse energies and the distance between the focusing lens and the sample are displayed in inserts.

However, in a higher fluence range (up to several hundreds of J/cm^2) this evolution law is no more obeyed. This can be easily observed on Fig. 3 d, where we used a much tighter focusing (~ 0.2 mm crater diameter) of the laser beam on the sample, by changing the distance between the lens and the sample from 20 cm to 25 cm. One can thus speculate on the transition to a new ablation regime, where the energy would be pulled by different processes (most probably multiple ionization) rather than used exclusively for thermal desorption.

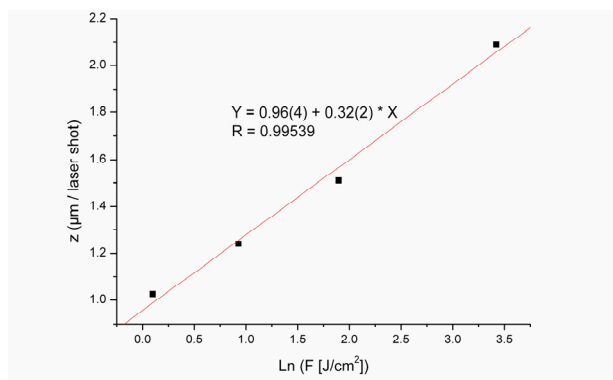
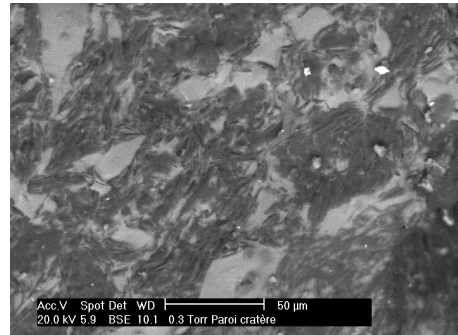
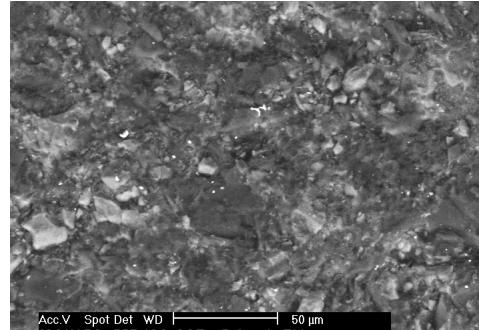


Fig. 4. Evolution of the ablation rate with the laser fluence.



a



b

Fig. 5. SEM micrographs of an irradiated zone (a) compared to a reference (non-irradiated) area of the sample surface (b).

The investigations of the modifications induced on the sample by laser exposure have been further continued by using a scanning electron microscope (Philips XL 40) in the CRMHT laboratory (Orléans). Fig. 5 presents a comparison of an irradiated area (crater, 30 J/cm²) with a non-irradiated zone of the sample surface. One can easily remark large modifications of the sample with irradiation according to microstructure and chemical composition (contrast). Thanks to an EDS (Energy Dispersive X-ray Spectroscopy) analysis, we can clearly identify a segregation of major phases with BN for the darkest grains, and SiO₂ for the lighter ones. The very light grains correspond to metals (Cu, Mn) originally present as impurities in the sample. We observe that the mean composition of the crater is impoverished in SiO₂, thus concluding on a loss of homogeneity in the crater due to the melting process induced by irradiation. In order to verify this statement, we have performed supplementary experiments by collecting the ejected material on a glass substrate (microscope slide) placed in vacuum at 45° with respect to the sample. The thin film deposited is under analysis at CMRHT. The results of these experiments will also permit a comparison with similar data obtained on deposits collected directly in the PIVOINE facility during a HET run.⁹

3.2 Optical and spectral investigations on the ablation plasma dynamics

In order to further characterize the results of the laser-sample interaction, we performed optical (ICCD camera) and spectral (monochromator) investigations of the UV and visible light emitted by the expanding plasma plume. As an example, Fig. 6 displays two ICCD images recorded at 200 ns and 700 ns delays after the laser pulse. These images reveal a splitting of the plasma plume in two structures. This splitting process has already been observed in studies on model targets as Cu,¹⁰⁻¹¹ Al,¹² or graphite,¹⁴ and has been numerically retrieved in the frame of a theoretical model based on fractal hydrodynamics.¹² From a chemical composition point of view, the generally accepted idea is that the first structure consists mainly in individual unit particles (atoms, ions, monomers), while the second one is formed of clusters and nanoparticles.^{15,16} The two structures exhibit distinct dynamics and velocities, usually in the range of 10⁴ m/s for the former and 10³ m/s for the latter [12]. For instance, using the data in Fig. 6, a velocity of 5.8×10³ m/s can be derived for the second structure (maximum emission point).

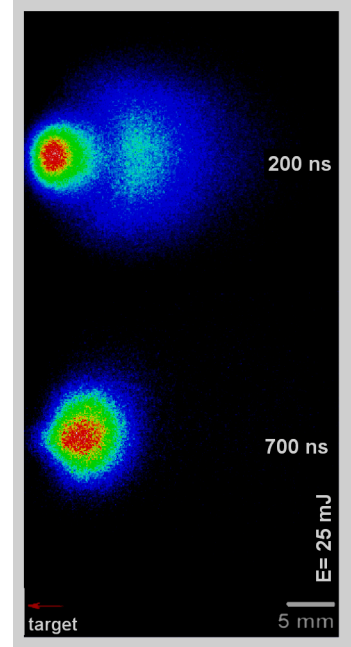


Fig. 6. ICCD images of the plasma plume dynamics.

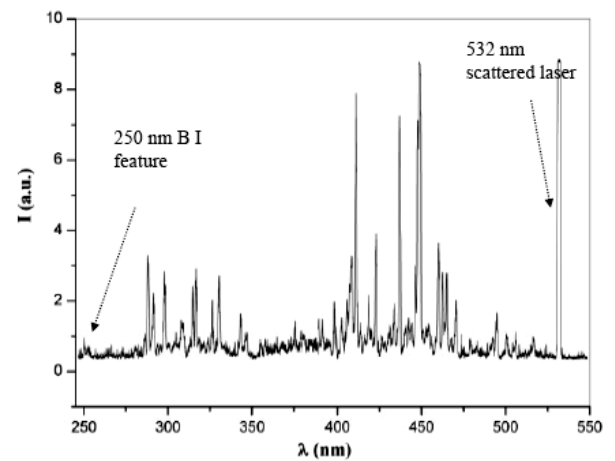


Fig. 7. Optical emission spectrum of the plasma created by ablation of BNSiO₂. Laser energy: 50 mJ/pulse, target – slit center distance: 0.5 mm.

Although these ICCD measurements can give a useful preliminary insight on the dynamics of the plasma plume as a whole, they cannot offer information on the individual contribution of each species present in this complex mixture. In order to separate these contributions, we have performed a spatio-temporal resolved spectroscopy study by using a monochromator and a fast response photomultiplier (PM). With the monochromator grating turning (typically at 20 nm/min speed) and the laser fired at 10 Hz, we transferred in real-time the transitory signals recorded by the PM to the LeCroy oscilloscope and used its “Trend” utility to monitor the peak intensity of the signals versus time, i.e. versus the monochromator grating

position. With the values above, one gets 30 measurements points (laser shots) per nm, which is largely enough when considering the resolution of the apparatus (~ 1 nm). Fig. 7 displays an overview of the 245 – 545 nm spectral region, recorded with a laser energy of 50 mJ/pulse in the immediate vicinity of the target (distance to slit center : 0.5 mm). The most prominent feature on the spectrum is the 532 nm line representing the laser scattered light (which can also be used as reference point). The wavelength scale has been calibrated using an Hg spectral lamp, with an accuracy of ± 0.3 nm.

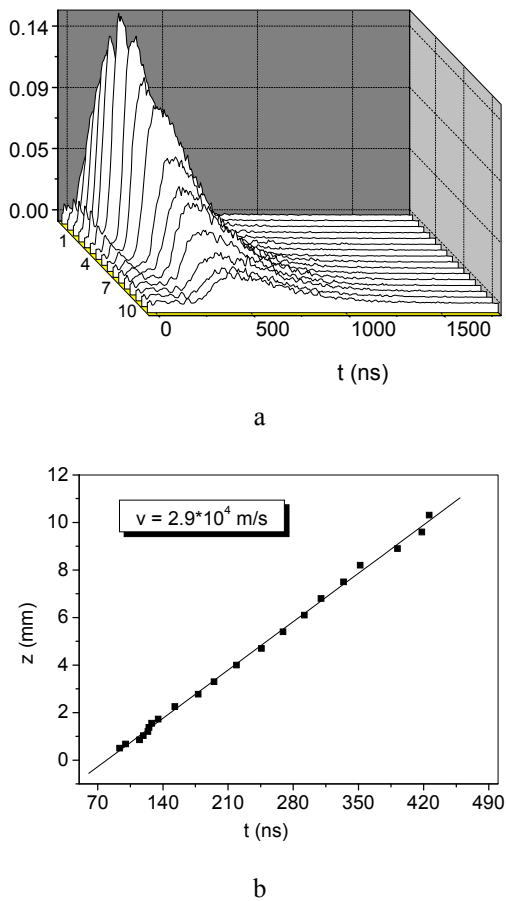


Fig. 8. a) Spatio-temporal evolution of the 250 nm spectral feature intensity (each temporal profile is averaged on 50 laser shots of 200 mJ/pulse energy); b) B I species velocity derived from a linear fit of the distance to the target against the time of maximum intensity.

The complete assignment of the spectral lines displayed in Fig. 7 is underway. For this preliminary stage, we focused our attention on the 250 nm feature which has been assigned to the well-known B I doublet $^2\text{P}_{1/2} - ^2\text{S}_{1/2}$ (249.67 nm) and $^2\text{P}_{3/2} - ^2\text{S}_{1/2}$ (249.77 nm).¹⁷ Note that these lines are currently used to monitor in-situ the erosion process affecting the dielectric walls of HETs. [7-8] This motivated us in a more detailed study on the spatio-temporal behaviour of the 250 nm feature and the associated species. An experimental device has been developed to allow the translation of the target surface

with respect to the slit position (fixed) without changing the laser beam focusing (i.e. the lens – target distance). When varying the target – slit center distance in the 0.5 – 10 mm range (along the Z axis), we recorded the temporal intensity profiles (integrated over the sight XY plane), of the 250 nm spectral feature. These profiles are displayed in Fig. 8a. By representing the evolution of the maximum signal intensity time with respect to the distance from the target (Fig. 8b), one can derive the velocity of the maximum emission point (2.9×10^4 m/s in our case). Assuming that the optical emission intensity is representative of the species abundance (which seems to be supported by the linear law obtained), we can consider this value as being the velocity of the B I component in the expanding plasma, thus leading to a kinetic energy of ~ 50 eV for this species. This is comparable with typical values recorded in HETs (e.g. $\sim 2 \times 10^4$ m/s for sputtered boron⁷).

4. Conclusion

We presented in this paper preliminary results on the interaction between a laser beam and BNSiO_2 surfaces, in an effort to simulate the energy deposition on the annular chamber dielectric walls in HETs. The modifications induced by the laser irradiation on the solid sample have been investigated by profilometry and scanning electron microscopy. The plasma plume created by ejection of particles in the gas phase has also been studied by means of optical and spectral methods. These preliminary results seem encouraging and present a clear fundamental interest. Although the deposition of energy by pulsed laser beams seems at the moment to induce much more dramatical effects on the dielectric surface than those observed under normal working conditions for HETs (especially in terms of erosion rates), these tests could be representative of particular operating conditions. An alternative approach is under study in our laboratories, involving the use of high-power continuous wave lasers to selectively heat specific points on the sample surface. Depending on the results of these investigations, a possible implementation of the technique on the French PIVOINE facility is envisaged.

Acknowledgments

This research is supported by the French Research Group, GDR CNRS/CNES/SNECMA/Universités n°2759 "Propulsion Spatiale à Plasma". The Centre d'Etudes et de Recherches Lasers et Applications is supported by the Ministère chargé de la Recherche, the Région Nord-Pas de Calais and the Fonds Européen de Développement Economique des Régions.

References

[1] M. Karas, D. Bachmann, F. Hillenkamp, *Analytical Chemistry* **57**(14), 2935 (1985).

[2] M. Karas, D. Bachmann, U. Bahr, F. Hillenkamp, International Journal of Mass Spectrometry and Ion Processes **78**, 53 (1987).

[3] Pulsed Laser Deposition of Thin Films, edited by. D. B. Chrisey and G. K. Hubler, Wiley, New York, 1994.

[4] D. B. Chrisey, A. Piqué, R. A. McGill, J. S. Horwitz, B. R. Ringisen, D. M. Bubb, P. K. Wu, Chemical Reviews, **103**(2), 553 (2003).

[5] N. Gascon, M. Dudeck, S. Barral, Physics of Plasma, **10**(10), 4123 (2003).

[6] S. Barral, K. Makowski, Z. Peradzynski, N. Gascon, M. Dudeck, Physics of Plasma **10**(10), 4127 (2003).

[7] D. Pagnon, P. Lasgorceix, M. Touzeau, 4th Int. Spacecraft Propulsion Conference, ISPC 2004, Chia Laguna, Sardinia, Italy, 2-9 June 2004.

[8] D. Pagnon, M. Touzeau, P. Lasgorceix, 40th AIAA/ASME/SAE/ASEE Joint Propulsion Conference, Florida, July 2004

[9] D. Pagnon, S. Pellerin, P. Lasgorceix, C. Legentil, 30th International Electric Propulsion Conference, IEPC 2007-paper166, 16-20 September 2007, Florence, Italy.

[10] S. Gurlui, M. Sanduloviciu, C. Miheşan, M. Ziskind, C. Focsa, AIP Conference Proceedings, **812**, 279 (2006).

[11] S. Gurlui, M. Sanduloviciu, M. Strat, G. Strat, C. Miheşan, M. Ziskind, C. Focsa, J. Optoelectron. Adv. Mater. **8**(1), 148 (2006).

[12] S. Gurlui, M. Agop, P. Nica, M. Ziskind, C. Focsa, Phys. Rev. E, submitted, 2007.

[13] S. Georgiou, A. Koubenakis, Chemical Reviews, **103**(2), 349 (2003).

[14] N. M. Bulgakova, A. V. Bulgakov, O. F. Bobrenok, Physical Review E, **62**(4), 5624 (2000).

[15] M. Vitiello, S. Amoruso, C. Altucci, C. de Lisio, X. Wang, Applied Surface Science **248**(1-4), 163 (2005)

[16] S. Amoruso, R. Bruzzese, N. Spinelli, R. Velotta Vitiello, X. Wang, G. Ausanio, V. Iannotti, L. Lanotte, Applied Physics Letters **84**(22), 4502 (2004).

[17] NIST Atomic Spectra Database (version 3.1.2), [Online]. Available: <http://physics.nist.gov/asd3> [2007, August 22]. National Institute of Standards and Technology, Gaithersburg, MD.

*Corresponding author: Cristian.Focsa@phlam.univ-lille1.fr